Production of runaway electrons by negative streamer discharges

Chanrion, Olivier Arnaud; Neubert, Torsten

Published in:
Journal of Geophysical Research: Atmospheres

Link to article, DOI:
10.1029/2009JA014774

Publication date:
2010

Document Version
Publisher's PDF, also known as Version of record

JOURNAL OF GEOPHYSICAL RESEARCH, VOL. 115, A00E32, doi:10.1029/2009JA014774, 2010

Production of runaway electrons by negative streamer discharges

O. Chanrion[1] and T. Neubert[1]

Received 14 August 2009; revised 23 December 2009; accepted 5 January 2010; published 9 June 2010.

[1] In this paper we estimate the probability that cold electrons can be accelerated by an ambient electric field into the runaway regime, and discuss the implications for negative streamer formation. The study is motivated by the discovery of ms duration bursts of γ-rays from the atmosphere above thunderstorms, the so-called Terrestrial Gamma-Ray Flashes. The radiation is thought to be bremsstrahlung from energetic (MeV) electrons accelerated in a thunderstorm discharge. The observation goes against conventional wisdom that discharges in air are carried by electrons with energies below a few tens of eV. Instead the relativistic runaway electron discharge has been proposed which requires a lower threshold electric field; however, seed electrons must be born with energies in the runaway regime. In this work we study the fundamental problem of electron acceleration in a conventional discharge and the conditions on the electric field for the acceleration of electrons into the runaway regime. We use particle codes to describe the process of stochastic acceleration and introduce a novel technique that improves the statistics of the relatively few electrons that reach high energies. The calculation of probabilities for electrons to reach energies in the runaway regime shows that even with modest fields, electrons can be energized in negative streamer tips into the runaway regime, creating a beamed distribution in front of the streamer that affects its propagation. The results reported here suggest that theories of negative streamers and spark propagation should be reexamined with an improved characterization of the kinetic effects of electrons.

Citation: Chanrion, O., and T. Neubert (2010), Production of runaway electrons by negative streamer discharges, *J. Geophys. Res.*, *115*, A00E32, doi:10.1029/2009JA014774.

1. Introduction

[2] One of the most dramatic expressions of the electric discharge is lightning which can travel for tens of kilometers within a cloud, then strike to ground with a shattering force. The courageous experiments with lightning of Benjamin Franklin and Jacques de Romas in the 18th century led to discoveries of fundamental aspects of electricity; they began the journey of exploration into the phenomenon of the gas discharge: the "spark."

[3] After many years of research into atmospheric electric discharges there are still surprises. Consider the chance discovery in 1989 of discharges in the mesosphere at 50–80 km altitude above thunderstorms, now known as "sprites" [*Franz et al.*, 1990]. Although electrical breakdown between thunderclouds and the ionosphere was predicted by the Nobel laureate C. T. R. Wilson in 1925 [*Wilson*, 1925a] and anecdotal stories of flashes of light in the high-altitude atmosphere were published even earlier [*MacKenzie and Toynbee*, 1886], the discovery came as a surprise to scientists. Consider another chance discovery a few years later, in 1994, of ms duration bursts of γ-rays from the atmosphere above thunderstorms reaching energies above 300 keV. These Terrestrial Gamma-Ray Flashes (TGFs) were observed by detectors on the Compton Gamma Ray Observatory (CGRO) satellite designed to observe radiation from space [*Fishman et al.*, 1994]. It was soon proposed that the radiation must be bremsstrahlung from energetic electrons accelerated in the thunderstorm fields to relativistic energies. The mechanism considered most likely was the so-called relativistic runaway electron discharge [*Gurevich et al.*, 1992] first proposed by *Wilson* [1925b], where the electron avalanche is formed by high-energy electrons, although alternative suggestions like the relativistic feedback or the acceleration of cold electrons in strong electric fields have emerged recently [*Dwyer*, 2008]. The discovery of new phenomena above thunderstorms was topped in 2002 with observations of the longest electric discharge on planet Earth, reaching from thunderstorm clouds, through the stratosphere and mesosphere, to the bottom ionosphere at 90 km altitude [*Pasko et al.*, 2002].

[4] These discoveries have spawned many studies of the basic physics of discharges [e.g., *Neubert et al.*, 2008; *Ebert et al.*, 2010; *Pasko*, 2007, and references therein]. The aim has been to understand the new phenomena, their interrelationship and their dependence on the characteristics of the

[1]National Space Institute, Danish Technical University, Copenhagen, Denmark.

0148-0227/10/2009JA014774

thunderstorms below. In the paper presented here, however, we return to the fundamental problem of electron acceleration in streamers. Whereas X- and γ-rays have been observed in relation to thunderstorm activity under various circumstances and are assumed to be bremsstrahlung from energetic electrons, the electrons themselves have been poorly characterized, since the instrumentation generally has not been able to distinguish electrons from photons. However, the evidence of energetic electrons in discharges is convincing and points to electron acceleration as a key issue. In the past, this fundamental physical process has been difficult to describe because of the very large computational load required for good statistics on the electron distributions. The problem is attacked here with an electrostatic Particle-in-Cell code (PIC) with Monte Carlo Collisions (MCC) [*Chanrion and Neubert*, 2008]. The codes have been refined by an algorithm that allows characterization of the electron distribution in electric discharges with an unprecedented precision at high energies.

[5] In the following we first present a review of the experimental evidence for high-energy electrons in the atmosphere, which is followed by a description of the conventional discharge and the runaway discharge. Then we present a short description of the computational method. Finally we give some results on the electric field magnitudes needed for electron acceleration from the thermal to the relativistic regime and of the implications for streamer propagation.

2. Evidence for Relativistic Electrons in Discharges

[6] Since the first proposition of the runaway electron discharge from thundercloud tops to the ionosphere by Wilson, the search for evidence of the process has been conducted both with observations taken during thunderstorms and in the laboratory. Although early data suggested that energetic electrons were more abundant in thunderstorms than in the fair weather atmosphere, it was conjectured for many years that energetic electrons are unlikely in lightning discharges because of the absence of clear X- and γ-ray signatures from bremsstrahlung radiation. In laboratories, it was not until the 1960ies that X- and γ-rays from energetic electrons were observed, for large over-voltage discharges ($E \gg E_k$; see section 3) [*Babich et al.*, 2003].

[7] The first convincing report on the existence of energetic electrons in the atmosphere came in 1982 when X-rays from a few keV to above 12 keV were observed above thunderstorms from instrumentation on aircraft [*Parks et al.*, 1981]. The observations were repeated a few years later with NaI crystal sensors sensitive to energies above 100 keV, flown on an aircraft through thunderstorm clouds that was repeatedly struck by lightning [*McCarthy and Parks*, 1985]. Observations showed increased fluxes during a few seconds before a lightning discharge, at which time the fluxes fell abruptly to the background level. There was an absence of a one-to-one correlation, however, which was explained to result from different measurement positions relative to the active regions. Two mechanisms were suggested: the original idea of Wilson where the discharge is powered by relativistic electrons [*Wilson*, 1925a, 1925b; *Gurevich et al.*, 1992], and acceleration of cold electrons near the enhanced field regions of leader tips [*Gurevich*, 1961].

[8] Further discussions of the X-ray observations categorize mechanisms into those of a background field in a thunderstorm accelerating background electrons and those of high local electric fields at lightning streamer or leader tips accelerating cold electrons in the streamer/leader discharge. It was argued that the first mechanism is most likely and that the flux of energetic electrons created by cosmic rays was enhanced by secondary ionization and acceleration in the background electric field to the levels needed to explain the observations [*McCarthy and Parks*, 1985].

[9] During the 1990ies, observations of electric fields and X-rays (30–120 keV) were taken from balloons inside the stratiform region of a mesoscale convecting system. Here, two kinds of X-ray emissions were observed. One was pulses of X-rays of ~1 s duration, 1–2 orders of magnitude above the background. These were not seen to correlate with electric field activity and no plausible explanation was suggested [*Eack et al.*, 1996a]. The second observation was changes in X-ray radiation on timescales of the order of 1 min. The radiation and the electric field decreased abruptly at the time of a lightning discharge suggesting that the background cloud electric field was driving the process [*Eack et al.*, 1996b]. However, the field strength was found to be insufficient to explain the flux levels when compared to model estimates [*McCarthy and Parks*, 1992]. The end of the decade saw balloon observations of X-rays up to 300 keV and electric fields confirming previous findings, suggesting that the cloud field accelerates electrons to high energies, but not being limited to the main charge regions of a cloud [*Eack et al.*, 2000]. During the past 10 years several observations have been conducted from the ground of high-energy radiation lasting seconds to minutes and associated with thunderstorm activity [*Brunetti et al.*, 2000; *Torii et al.*, 2002; *Tsuchiya et al.*, 2007]. The observations confirm the view that thundercloud fields may enhance fluxes of energetic electrons to levels where bremsstrahlung can be detected and suggest that the dimension of the electric field source region is of the order of 100 m [*Torii et al.*, 2009; *Tsuchiya et al.*, 2009].

[10] Whereas the observations described above suggest effects of the large-scale cloud electric field on energetic electrons created by an external source of cosmic rays, the discovery in the 1990ies of ms duration flashes of X and γ radiation from the atmosphere above thunderstorms changed the picture. These Terrestrial Gamma-ray Flashes (TGFs) were observed by instrumentation on the Compton Gamma Ray Observatory (CGRO) satellite [*Fishman et al.*, 1994] and later confirmed by observations of the Reuven Ramaty High Energy Solar Spectroscopic Imager (RHESSI) [*Smith et al.*, 2005]. The new observations suggest that TGFs have energies extending up to at least 20 MeV and that the discharge itself must generate energetic radiation as in the relativistic runaway electron discharge process [*Gurevich et al.*, 1996; *Roussel-Dupre and Gurevich*, 1996]. Further evidence of energetic radiation from the lightning discharge came from observations of radiation up to 1 MeV in association with lightning striking nearby trees. The radiation began 1–2 ms before a lightning discharge connected to a tree and lasted until the onset of the first return stroke [*Moore et al.*, 2001]. More evidence came from an experiment with rocket triggered lightning, where the discharge path is along the conducting wire connecting the rocket with the ground [*Dwyer*

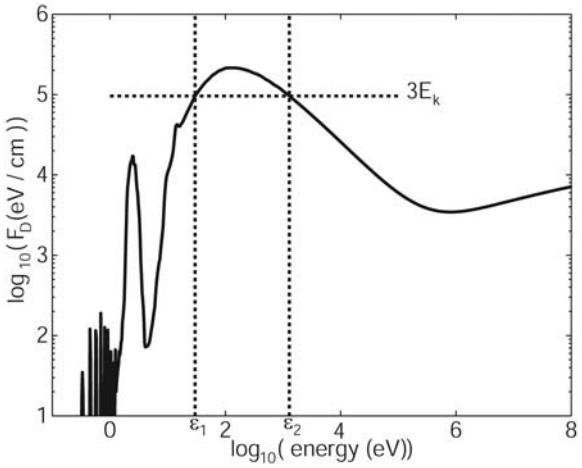

Figure 1. The frictional force in air composed of 80% N_2 and 20% O_2 at 1 atm pressure. The force corresponding to an electric field of $3E_k$ is also shown. The two forces are of equal magnitude for the energies ϵ_1 and ϵ_2.

et al., 2003]. A single burst of radiation with energies up to 10 MeV was seen during 300 μs corresponding to the initial phase of the rocket triggered lightning [*Dwyer et al.*, 2004]. Later experiments with 8 NaI detectors distributed around the rocket launch site confirmed the results. They found that X-rays and leader step electric field changes were colocated within 50 m [*Howard et al.*, 2008].

[11] Radiation from electric discharges is now also well established in laboratory experiments. Recent work has documented μs duration bursts of X-rays at 30–150 keV in 1.5–2.0 m sparks of 1.5 MeV. X-rays are observed during the high voltage part of the spark and during the collapse of the voltage, but not during the high-current arc. This is similar to lightning where energetic radiation is observed during the dart leader phase that bridges the cloud charge regions to the ground until the very beginning of the return current stroke [*Dwyer et al.*, 2005b]. The experiments have been continued, capturing photons above 300 keV and verifying past results [*Dwyer et al.*, 2008; *Nguyen et al.*, 2008].

[12] The energy spectra measured during rocket triggered lightning [*Dwyer*, 2004], natural lightning [*Dwyer et al.*, 2005b], and laboratory sparks [*Dwyer et al.*, 2005a] is not energetic enough to be consistent with the relativistic runaway electron avalanche multiplication theory in its original form where energetic seed electrons are created by cosmic rays. It has been suggested instead that a flux of keV electrons are generated from the leader or streamer tips of the discharge.

[13] From the above it is clear that the small-scale field region of discharges can be the source of ms duration bursts of energetic radiation. Energization of cold electrons in a discharge has been discussed by *Gurevich et al.* [2007], *Moss et al.* [2006], *Chanrion and Neubert* [2008], and *Li et al.* [2008b, 2009] and is studied in the present paper. Before we continue with a presentation of the results we first review some aspects of the electric discharge.

3. Energetics of Discharges

[14] It is useful to discuss the electric discharge in terms of the frictional force F_D of the medium acting on an electron. For the electron to gain energy ϵ the force F_E of the electric field must on average overcome the frictional force:

$$d\epsilon/dt = v(F_E - F_D) > 0 \quad (1)$$

where $F_E = qE\cos(\beta)$, v is the velocity of the electron, β the angle between the velocity vector and the electric field and q the charge of the electron (negative). The minimum electric field required for an electron to gain energy occurs when the electric field is directed opposite to the velocity vector ($\cos(\beta) = -1$). The frictional force on an electron in air at 1 atm pressure is shown in Figure 1. Electrons accelerated from low energies experience increasing friction until about ~100 eV where the frictional force reaches a maximum $F_{\max}$. At higher energies the friction decreases until ~1 MeV where the increasing relativistic mass again increases the force.

[15] The most common streamer discharges in gases are sometimes called "thermal" discharges, where electrons are well below the energy corresponding to the maximum frictional force and the electric field is close to, but above, the magnitude needed to sustain the discharge. In the thermal discharge the high-energy tail of the electron distribution is above the ionization threshold (~15 eV for N_2) and supports the ionization avalanche. However, electrons reaching energies above ~100 eV are usually considered to be negligible. The threshold electric field for the thermal discharge is defined as the field where the ionization rate in the electron avalanche equals the loss rate, which is primarily through electron attachment to neutral gas constituents. The threshold field measured in laboratory experiments is found to depend on the experimental configuration, for instance the electrode gap length, the electrode material and their geometric shape. In air at 1 atm pressure, the threshold field is ~32 kV cm^{-1} for short gaps, falling to ~26 kV cm^{-1} for long gaps [*Raizer*, 1991]. Because the threshold field is proportional to N, the number density of atmospheric molecules, it is sometimes expressed as the so-called reduced field $E_k = E/N$. This is often given in units of the "Townsend" defined as 1 Td = 10^{-17} V cm^2. As the number density of air at 1 atm pressure is ~2.7×10^{19} cm^{-3}, the above threshold fields correspond to 119 Td and 96 Td, respectively. In the following we use the definition consistent with the theoretical Townsend condition which is ~32 kV cm^{-1} and 119 Td.

[16] The minimum electric field required to overcome the maximum of the frictional force $F_{\max}$ at ~100 eV is about $E_{\max} \sim 7.5\, E_k$. When such fields are present, any electron may experience continued acceleration to relativistic energies [*Babich*, 2003]. Figure 1 shows the force F_E from an electric field equal to 3 E_k acting on an electron with a velocity antiparallel to the field ($\cos(\beta) = -1$). The electric and frictional forces are equal at energies $\epsilon_1 = 29.9$ eV and $\epsilon_2 = 1288$ eV. The equilibrium at $\epsilon = \epsilon_1$ is stable with electrons at lower energies being on average accelerated and with electrons at higher energies, but below ϵ_2, being on average decelerated. The equilibrium at $\epsilon = \epsilon_2$ is unstable with electrons at higher energies being on average accelerated to around several tens of MeV, where a third equilibrium (not shown) is found. These are the runaway electrons predicted by Wilson.

4. PIC-MCC Code With Adaptive Particles

[17] The framework described above of an average frictional force is useful for understanding some of the basic

physical concepts. However, the process is really stochastic, as an electron in any field has a finite chance of being accelerated into the runaway regime. To study electron acceleration further, a Particle-in-Cell (PIC) simulation code with a Monte Carlo Code (MCC) for collisions [*Chanrion and Neubert*, 2008] has been extended with an improved description of high-energy electrons.

[18] The codes were modified to take into account the relativistic electron mass increase by solving for electron momentum instead for velocity and by extrapolating cross sections to energies up to 100 MeV following the method given by *Graham and Roussel-Dupré* [1988] and *Murphy* [1988]. The scattering angle after a collision event is derived from measurements of both the total cross section and the momentum transfer cross section in N_2 given by *Okhrimovskyy et al.* [2002], to ensure a good approximation of the average scattering angle after collision. The energy is shared between the primary and secondary electrons during ionization according to *Opal et al.* [1971].

[19] Then an adaptive resampling scheme of computer particles was developed to improve the characterization of high-energy electrons. In the standard PIC methodology [e.g., *Chanrion and Neubert*, 2008, and references therein] computer particles represent many real electrons, described by a weight assigned to a computer particle. The true electron distribution function is reconstructed from the ensemble of computer particles taking their weight into account. The basic idea is now to maintain the sampling precision of the distribution function independent of the electron energy. This is done by first considering a set of energy intervals $I_n = [\epsilon'_n; \epsilon'_{n+1}]$ defined such that the number of real electrons in the interval I_n is twice the number of real electrons in I_{n+1}. The probability of finding a real electron in the first interval I_0 is then ~0.5, in interval I_1 = ~0.25, and so forth. The probability of the last interval is such that the total probability summed over all intervals equals 1. These $N_{\max}$ intervals are calculated from the distribution function of real electrons at a given time, with $\epsilon'_0 = 0$, $\epsilon'_{N\max+1} = +\infty$. $N_{\max}$ is determined implicitly in this scheme. Then the computer particles are split into 2 (or coalesced) such that the weight of computer particles in the interval I_n is twice as large as in I_{n+1} which then gives approximately the same number of computer particles in each energy bin in each cell. When computer particles have been advanced 10 PIC iterations they are split into two if they are accelerated from one energy bin into the bin above or coalesced if they are decelerated into energy bins below. The energy intervals are also recalculated every 10 PIC iterations with adjustments of a few computer particle weights. Any sequence of energy intervals can in principle be chosen, however, since particles are either coalesced or split in half, the sequence chosen is the simplest to implement. The above scheme is implemented after a run time when computer particles have begun to react significantly to the acceleration of the electric field, typically after a few hundred iterations. The particle resampling is implemented with the following rules:

[20] 1. If a computer particle has gained energy from an interval I_n to I_{n+1} it is split into two and the two new computer particles maintain the same particle velocity and position as the original one. Their weight is halved to conserve electron density and energy.

[21] 2. Computer particles that have lost energy are merged two by two if located within the same cell and energy bin. Merging is repeated until the particles of a cell and energy bin have a weight corresponding to those of the energy bin or as close as possible to, but below, that. The calculation of the position and the velocity of the merged particles follows *Chanrion and Neubert* [2008]. When the number of intervals is expected to become large, the particles that are to be coalesced can be thrown away instead in order to save computer time. This alternative was used to calculate the distribution function for 1.5 E_k, 2.25 E_k and 3 E_k presented in section 5.

[22] This resampling scheme is completed by a resampling similar to the one used by *Chanrion and Neubert* [2008] to limit the total number of computer particles.

[23] In past studies of discharges using particle codes [e.g., *Raju and Jianfen*, 1995a, 1995b, and references therein], different techniques of resampling were used to limit the number of computer particles. To the knowledge of the authors it is the first time that a resampling scheme has been devised for a PIC code with the purpose to increase the particle resolution with energy. The technique gives a uniform sampling of the logarithmic particle distribution over the complete energy range of the electrons. In the works of *Chanrion and Neubert* [2008], *Li et al.* [2008a], and *Li and Pitchford* [1989], resampling was used to limit the number of computer particles. In the simulations each particle have an equal probability to be coalesced. As a consequence the sampling precision decreased with the number density of real electrons. In the works of *Kunhardt and Tzeng* [1986] and *Moss et al.* [2006] this uniform remapping is performed in 3 and 2 energy intervals respectively, with a different resampling weight in each interval. This allows improvement the sampling precision in the high-energy tail of the distribution by a factor of 2 at most. This contrasts our method that keeps improving the sampling precision from interval to interval by a factor 2. Although it is beyond the scope of this paper to present a detailed numerical analysis of the method, we mention that the 1-D swarm simulations presented in section 5 gives confidence in the method for the studies of the problem of runaway electrons.

5. Electron Energy Distribution in 1-D Swarm Simulations

[24] The algorithm was first tested in one spatial dimension, undertaken to estimate the probability to obtain runaway electrons in a constant electric field in air. The simulation is performed using a swarm of computer electrons starting at rest and drifting in the electric field. The electrons undergo collisions and ionize the gas, but the electric field is not updated from the space charge fields. The number of computer particles is up to 4 millions. Photoionization is not included in order to better pinpoint the effect of the improved algorithm. The normalized electron distribution function f_e was determined for fields varying from 1.5 to 12 E_k. The results are shown in Figure 2. On the top horizontal axis is shown the energy from 1 eV to 20 keV, and on the right vertical axis is shown the normalized distribution function from 10^{-100} to 1. The distribution function has been determined over this remarkable range by allowing computer particles to represent any number of real particles down to a

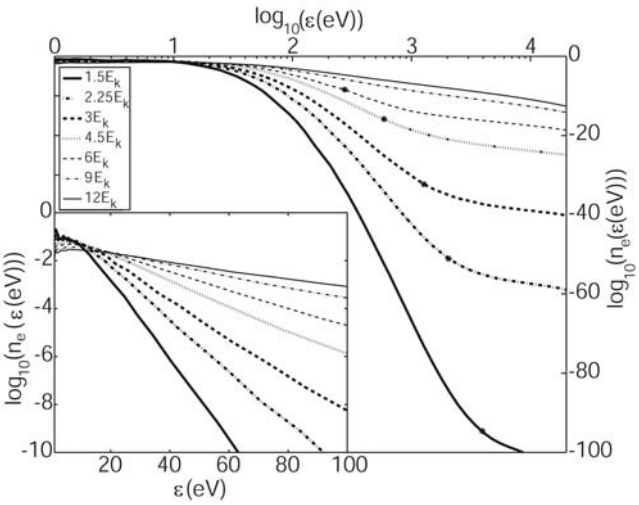

Figure 2. Swarm calculation of the normalized distribution function of electrons drifting in air in a constant electric field $E = 1.5\ E_k$ to $12\ E_k$. There is no photoionization, and the simulation is independent of the air pressure. The composition is assumed to be 80% N_2 and 20% O_2. The stars indicate the energy threshold ϵ_2 for each electric field.

fraction of a particle. Thus, the number of real particles that a computer particle represents is just a parameter and the functions are probabilities rather than normalized distributions of a realistic population of electrons. The insert is a blow-up of the distribution function for energies below 100 eV. The distribution functions have been compared to those of *Chanrion and Neubert* [2008] where energies up to a few hundred eV could be estimated, depending on the value of the background electric field. In this energy range there is an excellent agreement which gives confidence in the adaptive particle scheme.

[25] Moreover, it is interesting to note the robustness of the method. For instance, the distribution function obtained for a field of $1.5E_k$ shows detailed structures in the energy range below 100 eV. These were also found for electric fields below $2.5E_k$ by *Chanrion and Neubert* [2008], yet can reconstruct smoothly the distribution function up to 10 keV, reaching extremely small probabilities of the order of 10^{-100}.

[26] The runaway threshold energy ϵ_2 is shown as stars on the corresponding curves for different background electric fields. As seen from Figure 2, the threshold energy decreases with increasing electric field. We note that for those distribution functions where the electric field is below $E_{\max}$ and ϵ_1, ϵ_2 are defined, the slope changes around the runaway threshold energy as expected, being steeper at energies below and less steep at energies above. The high-energy tail is the "runaway branch" of the distribution.

[27] From these curves, the probability for electrons to exceed the threshold energy for runaway $P_e(\epsilon > \epsilon_2(E))$ has been calculated by integrating the distribution function above the runaway threshold ϵ_2. The result is presented in Table 1. The probability is 1 for electric fields above $E_{\max}$, and decreases dramatically as the field decreases below $E_{\max}$. This is a combined effect of the increase of the runaway threshold energy (see Figure 1) and the increasing difficulty of accelerating electrons with decreasing electric fields.

[28] The probabilities of Table 1 can be compared to the precision limit of a standard PIC-MCC. With the number of computer particles limited to the order of 10^7, achievable with contemporary computers, the precision of the probabilities is of the order of 10^{-7}. The lack of accuracy of the standard method becomes clear if we consider 10^{12} real electrons drifting in a field of $5.5E_k$. The probability for an electron to be in the runaway regime is then 7.4×10^{-10} and we obtain 740 real runaway electrons, but likely no computer particles in such a standard PIC-MCC simulation.

6. Simulation of Streamer Propagation in the Atmosphere

[29] In the work of *Chanrion and Neubert* [2008] we discussed the formation and initial propagation of a negative streamer simulated without an adaptive particle scheme. In the following we reproduce the same simulation, but use adaptive computer particles. The code is a two-dimensional, cylindrically symmetric, electrostatic PIC-MCC. The electric field E is given on a Cartesian grid and the computer particles are electrons that are allowed to be located anywhere in the simulation domain. The computer particles are moved and accelerated according to their velocities and the electric field interpolated to their positions. The Monte Carlo scheme determines whether electrons undergo collisions and the associated scattering, energy loss, attachment and ionization. The adaptive resampling scheme presented in section 4 is applied, but only for computer particles that represent more than one real electron. The mobility of ions is 2 orders of magnitude lower than the one of electrons and ions are therefore assumed to be motionless during the short time period of the simulations. Such assumptions are commonly used in discharge simulations [e.g., *Liu and Pasko*, 2004; *Kulikovsky*, 2000]. The electric field is updated from the space charge distribution.

[30] The neutral atmosphere consists of 80% N_2 and 20% O_2, the density is 1.61×10^{15} m^{-3}, corresponding to an altitude of 70 km, the background electric field is $E_o = 3E_k$ ($\epsilon_2 =$ 1288 eV) and the simulation is performed without photoionization. The domain corresponds to 52.5 m along the radius of the cylinder r and 420 m along the axis of the cylinder z, represented by 150 × 1200 cells. The number of computer particles may reach 50 million.

[31] Following *Liu and Pasko* [2004], the streamer is initiated from a plasma cloud of ionization with electrons and

Table 1. The First Equilibrium Energy ϵ_1, the Runaway Threshold ϵ_2, and the Probability for an Electron to Be in the Runaway Regime $P_e(\epsilon > \epsilon_2)$ as a Function of the Reduced Background Electric Field E/E_k[a]

E/E_k	ϵ_1 (eV)	ϵ_2 (eV)	$P_e(\epsilon > \epsilon_2)$
1.5	18.4	3926	1.6×10^{-93}
2.25	23.7	2077	5×10^{-50}
3	28.6	1288	4×10^{-31}
4.5	42.0	598	4.1×10^{-15}
5	48.1	470	3.6×10^{-12}
5.5	54.9	374	7.4×10^{-10}
6	62.7	277	9.4×10^{-8}
9	-	-	1
12	-	-	1

[a]The pressure is 1 atm, and the composition is 80% N_2 and 20% O_2.

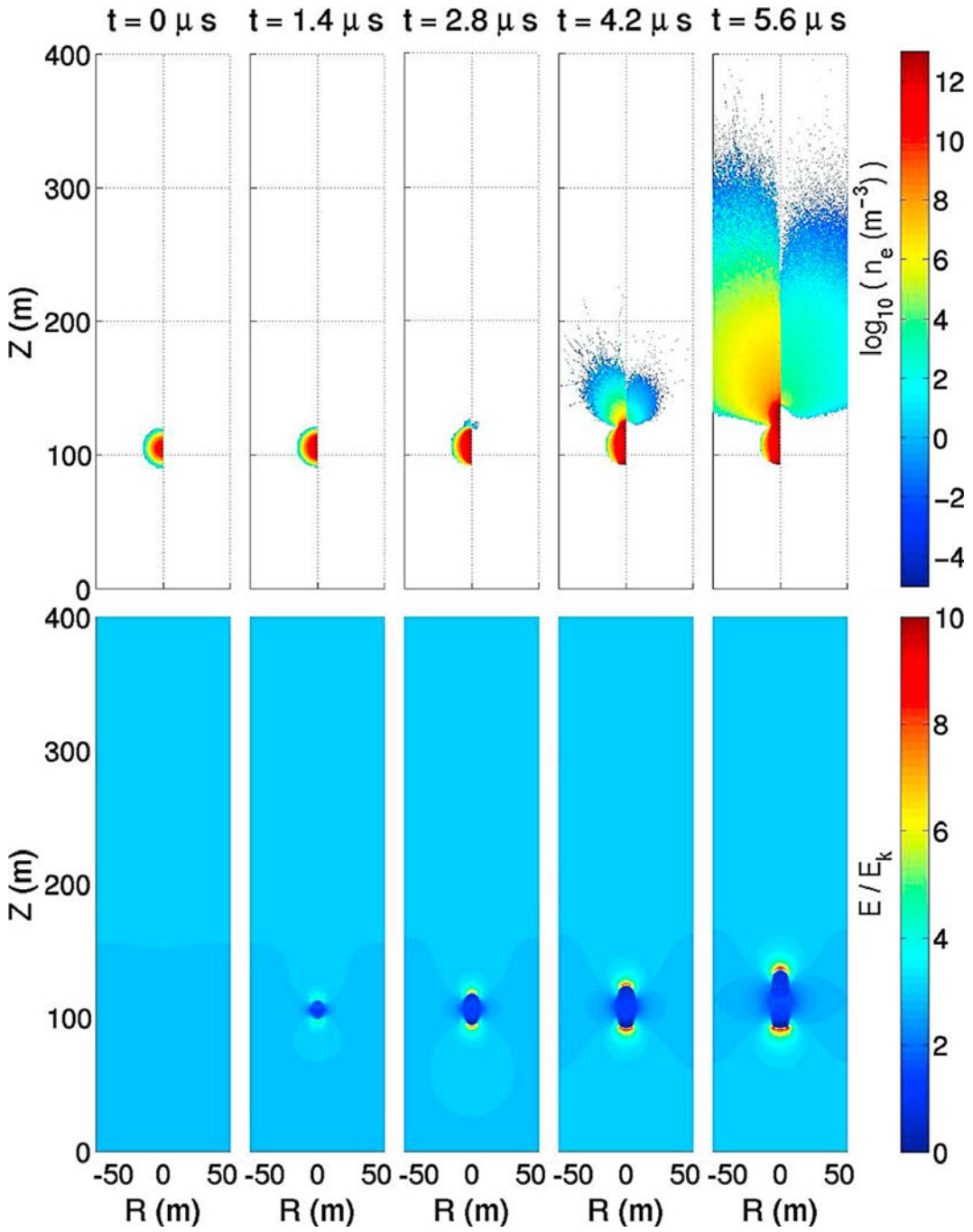

Figure 3. (top) Electron density and (bottom) electric field at different times up to 5.6 μs for a streamer propagating in air consisting of 80% N_2 and 20% O_2. The neutral gas density is 1.61×10^{15} m^{-3}, corresponding to an altitude of 70 km, and the background electric field is $E_o = 3\ E_k$. On the left half of each plot (Figure 3, top) are shown the total densities, and on the right half are shown the densities of real electrons in the runaway regime in the background electric field (energies above ϵ_2 = 1288 eV.)

ions at rest, identically to *Chanrion and Neubert* [2008]. The initial plasma cloud has a peak density of 5×10^{11} m^{-3} and a Gaussian spatial distribution with scale 3 m. In Figure 3 (top) are shown the real electron densities in the simulation domain at different times during the simulation, starting with the initial condition at $t = 0$. On the left half of each plot (Figure 3, top) are shown the total densities, and on the right half are shown the densities of real electrons with energies above ϵ_2 = 1288 eV. The magnitude of the densities given by the color scale is in units of $m^{\{-3\}}$. Figure 3 (bottom) shows the corresponding magnitudes of the electric field in units of V $m^{\{-1\}}$. The background field is directed downward, accelerating electrons upward. The movement of the electrons creates a negative space charge sheath at the top and a positive sheath of surplus ions at the bottom. Once the charge differences are high enough in the sheaths to distort the background field

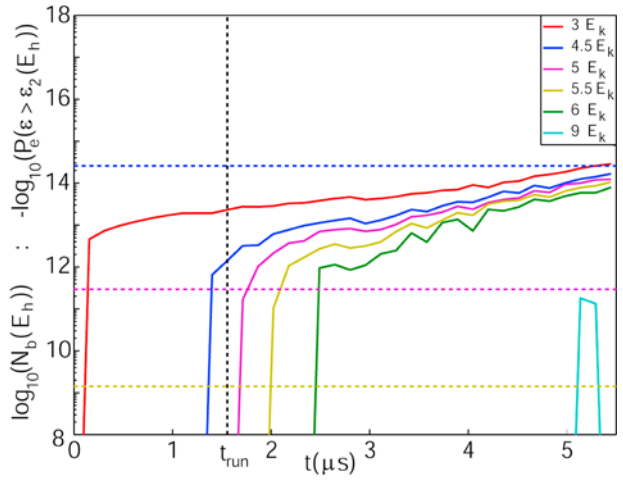

Figure 4. The number of real electrons $N_b(E_h)$ in regions of $E > E_h$ for $E_h/E_k = 3$, 4.5, 5, 5.5, 6, and 9 (solid curves) and the corresponding inverse probability $1/P_e(\epsilon > \epsilon_2(E_h))$ as dashed lines for $E_h/E_k = 4.5$, 5, and 5.5. The time t_{run} marking the first appearance of a runaway electron is indicated as a vertical black dashed line.

the streamer is formed. The downward directed positive streamer does not propagate because the photoionization process is not included and because there is no background ionization to form ionization avalanches below the tip. The upward directed negative streamer propagates with the electrons. Inside the streamer the electron density reaches $\sim 10^{12}$ m^{-3} which partially neutralizes the field inside.

[32] When discussing electron acceleration, the important driver is the local electric field acting on an electron. The electric field shown in Figure 3 is normalized to the conventional breakdown field E_k in order to demonstrate how the field in the streamer tip is enhanced above the background level by the thin layers of space charge in the tip. Usually, these fields allow a streamer, once formed, to propagate into regions of background fields below the Townsend breakdown field by bringing the local field in the tip above E_k. For positive streamers the background threshold field for propagation has been estimated to be $E_k^+ \sim E_k/6$ and for negative streamers $E_k^- \sim E_k/2.5$ [*Raizer*, 1991]. However, the values depend on the medium, the electrode geometry and many other parameters. This suggests field enhancement factors of ~6 and ~2.5, respectively. Moreover, the field enhancement in streamers is not well studied, partly because it is difficult to measure on the short timescales involved (ns at 1 atm pressure).

[33] Figure 3 shows that electrons are accelerated in front of the negative streamer tip, so forming a region of low-density electrons reaching to the top of the simulation domain by the end of the run. This region is formed by electrons that are accelerated in the streamer tip electric field enhancement to move ahead into the region of lower background electric field. In the process they gain energies above the runaway threshold also for the lower background field. As they move through the atmosphere they create ionization, with the secondary electrons predominantly with energies below the threshold energy for runaway. The low-density region has propagated between the last two time frames at an average speed of 0.3 c. This corresponds to an electron energy of 28 keV which is consistent with the maximum energy of electrons observed at the end of the run being 171 keV. The fact the electron density resulting from the flow of runaway electrons is not maximum on the axis far from the tip probably comes from an artifact of the cylindrically symmetric model. This question has not yet been analyzed, however, the high-density electron distribution in the streamer tip and the resulting electric field distribution are well behaved. The low electron density created by runaway electrons far above the tip is small and does not affect the electric field distribution.

[34] The question now is: at what electric field do the first runaway electrons appear in a negative streamer? In preceding work the field needed to obtain runaway electrons was assumed to be above the field corresponding to the maximum frictional force, $E_{max} = 7.5\ E_k$. However, with our high-precision description of the stochastic acceleration process, the first electron having an energy above the threshold energy for runaway appears at a time of $t_{run} = 1.55\ \mu$s when the maximum field enhancement in the negative tip is 4.9 E_k, a significantly lower value. The lower threshold can be understood from the discussion of the probabilities in section 5: the first runaway electron probably appears around the first time that a region is formed in the tip where the electric field magnitude exceeds a value E_h, and the number of electrons in the region $N_b(E_h)$ is such that $N_b(E_h) \times P_e(\epsilon > \epsilon_2(E_h)) \sim 1$. It is to be noted that the positive tip is insignificant in the observed flow of runaway electrons. Although the electric field is high, the electron number is small in the positive tip and any one that candidate to runaway is quickly decelerate in the streamer body where the field is reduced.

[35] The evolution in time of $N_b(E_h)$ with E_h/E_k at values between 3 and 9 is shown in Figure 4 (solid curves). Also shown is the inverse of the probability $P_e(\epsilon > \epsilon_2(E_h))$ for E_h/E_k at 4.5, 5 and 5.5 (dashed lines). The above criterion is fulfilled when the solid curve crosses the corresponding dashed curve (same color). This is realized first for $\sim 6.5 \times 10^{11}$ electrons drifting in a field of magnitude above 5 E_k (in purple) at a time 1.75 μs. This is in good agreement with the time $t_{run} = 1.55\ \mu$s at which the first electron in the runaway regime appears in the simulation. We note that, for such a density and electric field, the first runaway electron(s) may appear below the limit of precision of a standard MCC, which is ~4 orders of magnitude above the precision of the probability $\sim 1.5 \times 10^{-12}$ needed here. This may explain why other authors may have missed the first runaway electrons and why they needed higher field enhancement for runaway electron generation [*Babich*, 2003; *Chanrion and Neubert*, 2008].

[36] Figure 5 compares the simulation to one without energy-dependent resampling of the computer particles. On the left part of the plots are the real electron densities represented by the simulation without resampling of computer particles, and on the right part is the one already discussed, which includes resampling. The plots are close-ups to show the regions around the tips in more detail. Figure 5 (top) is for the time $t = 1.6\ \mu$s, and Figure 5 (bottom) is for $t = 5.4\ \mu$s. In the simulation with the standard PIC-MCC presented on the left the first runaway electron appears at $t = 3.4\ \mu$s when the maximum electric field enhancement in the negative streamer tip is $8E_k$. The streamer begins to branch because a low number of runaway computer particles represent a large number of real electrons. The computer particles

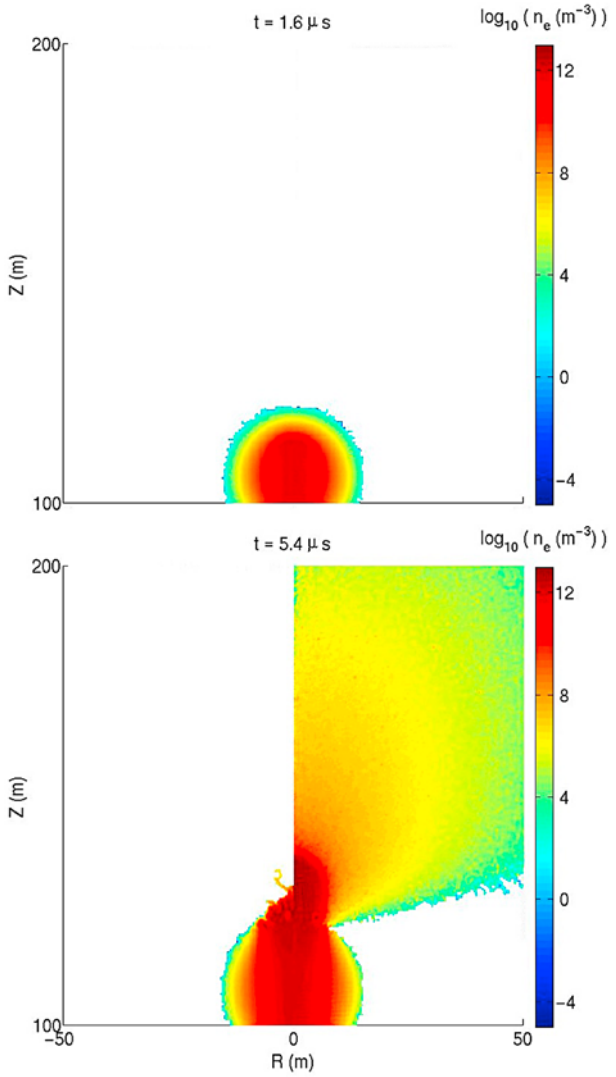

Figure 5. The electron density at (top) $t = 1.6$ μs and (bottom) $t = 5.4$ μs for the simulation presented in Figure 3 performed with the energy-dependent resampling of electrons (at right) and without (at left).

then create artificially enhanced ionization in their path. This nonadaptive simulation reproduces the features presented earlier by *Chanrion and Neubert* [2008]. In the simulation with adaptive computer particles, the first runaway electrons appear much earlier at $t = 1.55$ μs and at a weaker maximum field enhancement of 4.9 E_k. The number of computer particles accelerated ahead of the streamer is now relatively high because each represents a lower number of real electrons, thus creating a more uniform region in front of the tip. The electrons are beamed, with the higher-energy electrons being progressively more upward moving, while creating low-energy secondaries.

7. Discussion

[37] We have implemented an algorithm for energy-dependent resampling of electrons in a PIC-MCC. It has allowed us to investigate the stochastic acceleration of electrons with unprecedented precision and to estimate the probabilities of cold electrons to be accelerated into the runaway regime for a range of background electric fields, well below $E_{max} = 7.5$ E_k in air. The simulations presented show that the magnitude of the electric field needed for thermal streamers to produce runaway electrons is smaller than suggested by other studies published in the past [*Babich*, 2003]. Our results are evident, however, when one considers the stochastic nature of the acceleration process where, in principle, there is a finite probability that a cold electron will be accelerated into the runaway regime, even at field values approaching E_k.

[38] A similar conclusion was reached by *Li et al.* [2009] where the problem of electron acceleration was simulated using a fluid code for the body of the high-density streamer coupled with a particle code for the energetic electrons moving ahead of the streamer. However, in contrast to our results, only a few electrons were reported with energies in the runaway regime in the background electric field. Further studies are needed to resolve the differences in the two approaches.

[39] The probabilities shown in Table 1 can be used to evaluate whether a standard PIC-MCC is sufficient for studies of electron acceleration in discharges or whether the adaptive method presented here (or a similar method) must be used to resolve the statistics. The choice of method depends on the field magnitude and the number of electrons in the region of high electric field, as discussed in section 5.

[40] The probabilities depend only weakly on the presence of Argon in the atmosphere. The difference in the frictional force between an atmosphere composed of 80% N_2 and 20% O_2 and one composed of 78% N_2, 21% O_2 and 1% Ar is within 5% for energies below 20 eV and below 0.5% for energies above 20 eV.

[41] Photoionization affects streamer formation and propagation. In air, photons emitted from excited N_2 may ionize O_2 which has a lower ionization threshold. Photons have weaker interactions with air than electrons; they can travel further before they are absorbed or ionize a molecule. Photoionization also affects the electric field magnitudes of streamer tips. In the early stage of streamer development it reduces the fields around the streamer tips because the mean free path of a photon is larger than that of an electron; thus the region of ionization is broadened [*Bourdon et al.*, 2007; *Liu et al.*, 2007; *Liu and Pasko*, 2006; *Chanrion and Neubert*, 2008; *Luque et al.*, 2007].

[42] Unlike most parameters of discharges, photoionization in air does not scale with the gas density because of increased quenching with density of the excited states of N_2 that lead to photoionization of O_2 [*Liu and Pasko*, 2006]. Photoionization is also reduced by the presence of water vapor which absorbs photons. The water vapor content of the atmosphere at 1 atm and 100% humidity is ~4% at 0°C and ~15% at 20°C. This amount of water vapor reduces photoionization at ~0.1–1 cm distance from the location of photon emission by 1–2 orders of magnitude [*Naidis*, 2006]. The combination of high water vapor content and high pressure at low altitudes then has the effect of minimizing photoionization at low altitudes. Therefore, the production of energetic electrons in thermal negative streamers is more likely at low altitudes. We note that in the work of *Chanrion and Neubert* [2008] a streamer simulation was presented with the same parameters as used here in section 6, but for 10 km altitude and with

photoionization included. Still a relatively high field enhancement of 7 E_k was reached with a similar number of electrons in the tip. Therefore, runaway electrons may have been missed only because they used the standard PIC-MCC without adaptive electrons.

[43] A high transient electric field is more likely to build up in the streamer region of a lightning leader than in the high-altitude discharges of sprites in the mesosphere as discussed by *Moss et al.* [2006] and *Gurevich et al.* [2007]. The conclusion is then, that if a thermal discharge is to generate TGFs it is more likely that the discharge is at a low altitude in connection with lightning activity. This is consistent with recent estimates of the source altitude of atmospheric γ-ray bursts which place it at low altitudes in, or just above, the thunderclouds [*Dwyer and Smith*, 2005; *Østgaard et al.*, 2008; *Grefenstette et al.*, 2008a].

[44] From the simulation presented in section 6 we find at a time 5.6 μs that the vertical flux of runaway electrons is maximal crossing the plane z = 140 m and is equal to 3.2×10^{15} $m^{-2}s^{-1}$. In the work of *Moss et al.* [2006] the flux escaping the tip was estimated to 4×10^{14} $m^{-2}s^{-1}$ at the same altitude. Rescaling this value to lightning altitude, and considering a total of 55 streamers in a streamer region of a lightning leader carrying a current of 100 A, the total flux of runaway electrons was estimated to be 10^{18} s^{-1}. Under the same assumptions, our model would have given 8×10^{18} s^{-1} which is in good agreement. *Gurevich et al.* [2007] developed a model of runaway production by conventional discharges within a lightning leader tip. They estimated the flux of runaway electrons escaping a leader tip to 0.3×10^{18} $m^{-2}s^{-1}$, also in good agreement with *Moss et al.* [2006] and our result. Estimating the amplification from relativistic runaway electron avalanche they obtain good agreement between lightning gamma emission and TGF characteristics reported by *Smith et al.* [2005].

[45] The discussion above has focused on thermal electrons accelerated in negative streamers into the runaway regime. As mentioned in the introduction, electrons are created directly in the runaway regime by cosmic ray collisions with the atmosphere. The question is: which discharge process is more important, the thermal process or the relativistic process? The results presented here suggest an interesting scenario where the two processes are coupled: the thermal discharge produces a beam of relativistic seed electrons that allow ignition of the relativistic discharge. Longer streamer simulations including the effects of photoionization, are required to explore this scenario further.

[46] **Acknowledgments.** The authors would like to thank the conveners of the fruitful AGU Chapman Conference on Effects of Thunderstorms and Lightning in the Upper Atmosphere. They acknowledge helpful discussions with Ute Ebert, Li Chao, and Michael Rycroft and thank the referees for valuable comments.

[47] Zuyin Pu thanks the reviewers for their assistance in evaluating this paper.

References

Babich, L. (2003), *High-Energy Phenomena in Electric Discharges in Dense Gases: Theory, Experiment, and Natural Phenomena*, *ISTC Sci. Technol. Ser.*, vol. 2, Int. Sci. and Technol. Cent., Moscow.

Babich, L., R. Il'kaev, K. Bakhov, and R. Roussel-Dupre (2003), Calculation of high-altitude optical phenomena above thunderclouds based on a mechanism with the participation of relativistic electron avalanche, *Dokl. Earth Sci.*, *388*(1), 106–109.

Bourdon, A., V. Pasko, L. N.Y., S. Celestin, P. Segur, and E. Marode (2007), Efficient models for photoionization produced by non-thermal gas, *Plasma Sources Sci. Technol.*, *16*, 656–678.

Brunetti, M., S. Cecchini, M. Galli, G. Giovannini, and A. Pagliarin (2000), Gamma-ray bursts of atmospheric origin in the mev energy range, *Geophys. Res. Lett.*, *27*, 1599–1602.

Chanrion, O., and T. Neubert (2008), A pic-mcc code for simulation of streamer propagation in air, *J. Comput. Phys.*, *227*(15), 7222–7245, doi:10.1016/j.jcp.2008.04.016.

Dwyer, J. R. (2004), Implications of X-ray emission from lightning, *Geophys. Res. Lett.*, *31*, L12102, doi:10.1029/2004GL019795.

Dwyer, J. R. (2008), Source mechanisms of terrestrial gamma-ray flashes, *J. Geophys. Res.*, *113*, D10103, doi:10.1029/2007JD009248.

Dwyer, J. R., and D. M. Smith (2005), A comparison between Monte Carlo simulations of runaway breakdown and terrestrial gamma-ray flash observations, *Geophys. Res. Lett.*, *32*, L22804, doi:10.1029/2005GL023848.

Dwyer, J. R., et al. (2003), Energetic radiation produced during rocket-triggered lightning, *Science*, *299*, 694–697.

Dwyer, J. R., et al. (2004), A ground level γ-ray burst observed in association with rocket-triggered lightning, *Geophys. Res. Lett.*, *31*, L05119, doi:10.1029/2003GL018771.

Dwyer, J. R., H. K. Rassoul, Z. Saleh, M. K. Uman, J. Jerauld, and J. A. Plumer (2005a), X-ray bursts produced by laboratory sparks in air, *Geophys. Res. Lett.*, *32*, L20809, doi:10.1029/2005GL024027.

Dwyer, J. R., et al. (2005b), X-ray bursts associated with leader steps in cloud-to-ground lightning, *Geophys. Res. Lett.*, *32*, L01803, doi:10.1029/2004GL021782.

Dwyer, J. R., Z. Saleh, H. K. Rassoul, D. Concha, M. Rahman, V. Cooray, J. Jerauld, M. A. Uman, and V. A. Rakov (2008), A study of X-ray emission from laboratory sparks in air at atmospheric pressure, *J. Geophys. Res.*, *113*, D23207, doi:10.1029/2008JD010315.

Eack, K., W. Beasley, W. Rust, T. Marshall, and M. Stolzenburg (1996a), Initial results from simultaneous observation of X rays and electric fields in a thunderstorm, *J. Geophys. Res.*, *101*(29), 637–640.

Eack, K., W. Beasley, W. Rust, T. Marshall, and M. Stolzenburg (1996b), X-ray pulses observed above a mesoscale convective system, *Geophys. Res. Lett.*, *23*(21), 2915–2918.

Eack, K., D. Suszcynsky, W. Beasley, R. Roussel-Dupre, and E. Symbalisty (2000), Gamma-ray emissions observed in a thunderstorm anvil, *Geophys. Res. Lett.*, *27*(2), 185–188.

Ebert, U., S. Nijdam, A. Luque, C. Li, T. Briels, and E. van Veldhuizen (2010), Review of recent results on streamer discharges and discussion of their relevance for sprites and lightning, *J. Geophys. Res.*, doi:10.1029/2009JA014867, in press.

Fishman, G., et al. (1994), Discovery of intense gamma-ray flashes of atmospheric origin, *Science*, *264*, 1313.

Franz, R. C., R. J. Nemzek, and J. R. Winckler (1990), Television image of a large upward electrical discharge above a thundertorm system, *Science*, *249*, 48–51.

Graham, G., and R. Roussel-Dupré (1988), Relativistic collision rate calculations for electron-air interactions., *Rep. LA-11288-MS*, Los Alamos Natl. Lab., Los Alamos, N. M.

Grefenstette, B., D. M. Smith, J. R. Dwyer, and G. J. Fishman (2008a), Time evolution of terrestrial gamma ray flashes, *Geophys. Res. Lett.*, *35*, L06802, doi:10.1029/2007GL032922.

Gurevich, A. (1961), On the theory of runaway electrons, *Sov. Phys. JETP*, *12*, 904.

Gurevich, A., P. Lebedev, G. Milikh, and R. Roussel-Dupre (1992), Runaway electron mechanism of air breakdown and preconditioning during a thunderstorm, *Phys. Rev. A*, *165*, 463–468.

Gurevich, A., J. Valdivia, G. Milikh, and K. Papadopoulos (1996), Runaway electrons in the atmosphere in the presence of a magnetic field, *Radio Sci.*, *31*(6), 1541–1554.

Gurevich, A., K. Zybin, and Y. Medvedev (2007), Runaway breakdown in strong electric field as a source of terrestrial gamma flashes and gamma bursts in lightning leader steps, *Phys. Lett. A*, *361*, 119–125.

Howard, J., M. A. Uman, J. R. Dwyer, D. Hill, C. Biagi, Z. Saleh, J. Jerauld, and H. K. Rassoul (2008), Co-location of lightning leader X-ray and electric field change sources, *Geophys. Res. Lett.*, *35*, L13817, doi:10.1029/2008GL034134.

Kulikovsky, A. (2000), The role of photoionization in positive streamer dynamics, *J. Phys. D Appl. Phys.*, *33*, 1514–1524.

Kunhardt, E., and Y. Tzeng (1986), Monte-Carlo technique for simulating the evolution of an assembly of particles increasing in number, *J. Comput. Phys.*, *67*(2), 279–289.

Li, C., U. Ebert, and W. Brok (2008a), Avalanche to streamer transition in particle simulations, *IEEE Trans. Plasma Sci.*, *36*, 910–911.

Li, C., U. Ebert, W. Brok, and W. Hundsdorfer (2008b), Spatial coupling of particle and fluid models for streamers: Where nonlocality matters, *J. Phys. D Appl. Phys.*, *41*, 032005.

Li, C., U. Ebert, and W. Hundsdorfer (2009), 3D hybrid computations for streamer discharges and production of run-away electrons, *J. Phys. D Appl. Phys.*, *42*, 202003.

Li, Y., and L. Pitchford (1989), Density rescaling procedure for Monte-Carlo simulations of electron transport, *Appl. Phys. Lett.*, *54*(15), 1403–1405.

Liu, N., and V. Pasko (2004), Effects of photoionization on propagation and branching of positive and negative streamers in sprites, *J. Geophys. Res.*, *109*, A04301, doi:10.1029/2003JA010064.

Liu, N., and V. Pasko (2006), Effects of photoionization on similarity properties of streamers at various pressures in air, *J. Phys. D Appl. Phys.*, *39*, 327–334.

Liu, N., S. Celestin, A. Bourdon, V. Pasko, P. Segur, and E. Marode (2007), Application of photoionisation models based on radiative transfer and the Helmholtz equations to studies of streamers in weak electric fields, *Appl. Phys. Lett.*, *91*, 211501.

Luque, A., U. Ebert, C. Montijn, and W. Hundsdorfer (2007), Photoionisation in negative streamers: Fast computations and two propagation modes, *Appl. Phys. Lett.*, *90*, 081501.

MacKenzie, T., and H. Toynbee (1886), Meteorological phenomena, *Nature*, *33*, 26.

McCarthy, M., and G. Parks (1985), Further observations of X-rays inside thunderstorms, *Geophys. Res. Lett.*, *12*, 393–396.

McCarthy, M. P., and G. K. Parks (1992), On the modulation of X-ray fluxes in thunderstorms, *J. Geophys. Res.*, *97*(D5), 5857–5864.

Moore, C., K. Eack, G. Aulich, and W. Rison (2001), Energetic radiation associated with lightning stepped-leaders, *Geophys. Res. Lett.*, *28*(11), 2141–2144.

Moss, G., V. Pasko, N. Liu, and G. Veronis (2006), Monte Carlo model for analysis of thermal runaway electrons in streamer tips in transient luminous events and streamer zones of lightning leader, *J. Geophys. Res.*, *111*, A02307, doi:10.1029/2005JA011350.

Murphy, T. (1988), Total and differential electron collision cross sections for O_2 and N_2, *Rep. LA-11288-MS*, Los Alamos Natl. Lab., Los Alamos, N. M.

Naidis, G. (2006), On photoionization produced by discharges in air, *Plasma Sources Sci. Technol.*, *15*, 253–255.

Neubert, T., et al. (2008), Recent results from studies of electric discharges in the mesosphere, *Surv. Geophys.*, *29*(2), 71–137.

Nguyen, A., C. V. van Deursen, and U. Ebert (2008), Multiple X-ray bursts from long discharge in air, *J. Phys. D Appl. Phys.*, *41*, 234012.

Okhrimovskyy, A., A. Bogaerts, and R. Gijbels (2002), Electron anisotropic scattering in gases: A formula for Monte Carlo simulations, *Phys. Rev. E*, *65*, 037402.

Opal, C., W. Peterson, and E. Beaty (1971), Measurements of secondary-electron spectra produced by electron impact ionization of a number of simple gases, *J. Chem. Phys.*, *55*(8), 4100–4106.

Østgaard, N., T. Gjesteland, J. Stadsnes, P. H. Connell, and B. Carlson (2008), Production altitude and time delays of the terrestrial gamma flashes: Revisiting the burst and transient source experiment spectra., *J. Geophys. Res.*, *113*, A02307, doi:10.1029/2007JA012618.

Parks, G., B. Mauk, R. Spiger, and J. Chin (1981), X-ray enhancements detected during thunderstorm and lightning activities, *Geophys. Res. Lett.*, *8*, 1176–1179.

Pasko, V. (2007), Red sprite discharges in the atmosphere at high altitude: The molecular physics and the similarity with laboratory discharges (topical review), *Plasma Sources Sci. Technol.*, *16*(S13–S29), 152–154.

Pasko, V., M. Stanley, J. Mathews, U. Inan, and T. Wood (2002), Electrical discharge from a thundercloud top to the lower ionosphere, *Nature*, *416*(6877), 152–154.

Raizer, Y. (1991), *Gas Discharge Physics*, Springer, Berlin, Germany.

Raju, G., and L. Jianfen (1995a), Simulation of electrical discharges in gases: Uniform electric fields, *IEEE Trans. Dielectrics Electr. Insulation*, *2*(5), 1004–1015.

Raju, G., and L. Jianfen (1995b), Simulation of electrical discharges in gases: Nonuniform electric fields, *IEEE Trans. Dielectrics Electr. Insulation*, *2*(5), 1016–1041.

Roussel-Dupre, R., and A. Gurevich (1996), On runaway breakdown and upward propagating discharges, *J. Geophys. Res.*, *101*(A2), 2297–2311.

Smith, D., L. Lopez, R. Lin, and C. Barrigton-Leigh (2005), Terrestrial gamma-ray flashes observed up to 20 MeV, *Science*, *307*(5712), 1085–1088.

Torii, T., M. Takeishi, and T. Hosono (2002), Observation of gamma-ray dose increase associated with winter thunderstorm and lightning activity, *J. Geophys. Res.*, *107*(D17), 4324, doi:10.1029/2001JD000938.

Torii, T., T. Sugita, S. Tanabe, Y. Kimura, M. Kamogawa, K. Yajima, and H. Yasuda (2009), Gradual increase of energetic radiation associated with thunderstorm activity at the top of Mt. Fuji, *Geophys. Res. Lett.*, *36*, L13804, doi:10.1029/2008GL037105.

Tsuchiya, H., et al. (2007), Detection of high-energy gamma rays from winter thunderclouds, *Phys. Rev. Lett.*, *99*, 165002.

Tsuchiya, H., et al. (2009), Observation of an energetic radiation burst from mountain-top thunderclouds, *Phys. Rev. Lett.*, *102*, 255003.

Wilson, C. (1925a), The electric field of a thundercloud and some of its effects, *Proc. Phys. Soc. London*, *37A*, 32D–37D.

Wilson, C. (1925b), The acceleration of β-particles in strong electric fields, such as those of thunderclouds, *Proc. Cambridge Philos. Soc.*, *37A*, 32D–37D.

O. Chanrion and T. Neubert, National Space Institute, Danish Technical University, Juliane Maries Vej 30, DK-2100 Copenhagen, Denmark. (chanrion@space.dtu.dk)